Cell Reports

Report

# IMP3 Stabilization of WNT5B mRNA Facilitates TAZ Activation in Breast Cancer

## Graphical Abstract

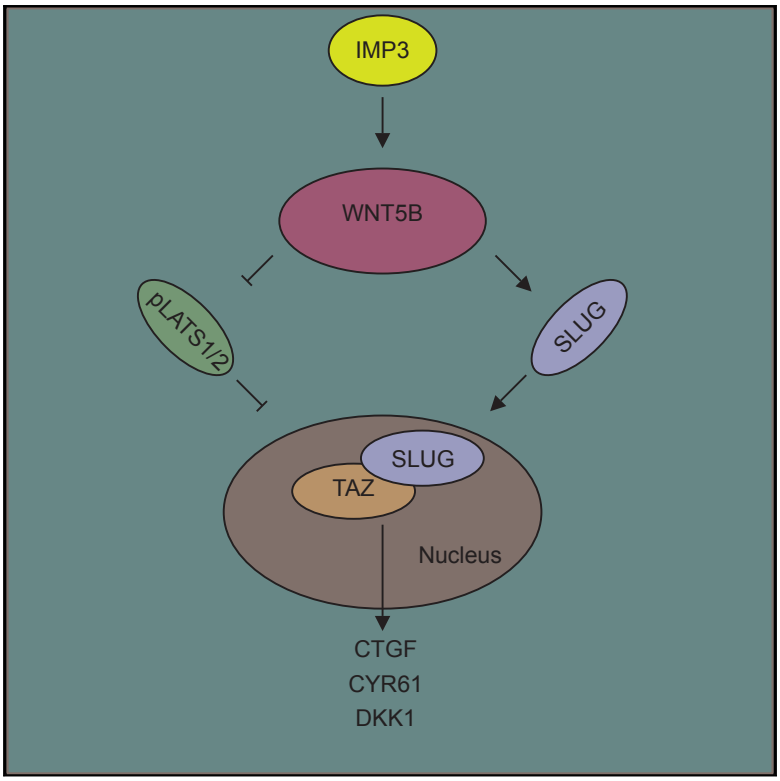


## Highlights

- IMP3 contributes to TAZ activation in breast cancer stem cells
- IMP3 stabilizes WNT5B mRNA and facilitates TAZ activation by alternative Wnt signaling
- IMP3 promotes WNT5B-mediated transcription of Slug, enabling TAZ nuclear localization
- TAZ activation by IMP3 involves integration of Hippo and alternative WNT signaling

## Authors

Sanjoy Samanta, Santosh Guru, Ameer L. Elaimy, ..., Jun Yu, Lihua J. Zhu, Arthur M. Mercurio

## Correspondence

arthur.mercurio@umassmed.edu

## In Brief

Mechanisms that regulate TAZ are critical for understanding the biology and improving the therapy of breast and other cancers. Samanta et al. demonstrate that insulin-like growth factor-2 mRNA-binding protein 3 (IMP3) contributes to TAZ activation in breast cancer stem cells by stabilizing WNT5B mRNA and facilitating alternative Wnt signaling. IMP3 and WNT5B also function together to promote the transcription of SLUG, which is necessary for TAZ nuclear localization and activation.

## Data and Software Availability

GSE107564

Samanta et al., 2018, Cell Reports *23*, 2559–2567
May 29, 2018 
https://doi.org/10.1016/j.celrep.2018.04.113

CellPress

Cell Reports
Report



# IMP3 Stabilization of WNT5B mRNA Facilitates TAZ Activation in Breast Cancer

Sanjoy Samanta,[1] Santosh Guru,[1] Ameer L. Elaimy,[1] John J. Amante,[1] Jianhong Ou,[1] Jun Yu,[1] Lihua J. Zhu,[1,2,3] and Arthur M. Mercurio[1,4,*]

[1]Department of Molecular, Cell and Cancer Biology, University of Massachusetts Medical School, 364 Plantation Street, Worcester, MA 01605, USA
[2]Department of Molecular Medicine, University of Massachusetts Medical School, 364 Plantation Street, Worcester, MA 01605, USA
[3]Department of Bioinformatics and Integrative Biology, University of Massachusetts Medical School, 364 Plantation Street, Worcester, MA 01605, USA
[4]Lead Contact
*Correspondence: arthur.mercurio@umassmed.edu
https://doi.org/10.1016/j.celrep.2018.04.113

## SUMMARY

**Insulin-like growth factor-2 mRNA-binding protein 3 (IMP3) is an oncofetal protein associated with many aggressive cancers and implicated in the function of breast cancer stem cells (CSCs). The mechanisms involved, however, are poorly understood. We observed that IMP3 facilitates the activation of TAZ, a transcriptional co-activator of Hippo signaling that is necessary for the function of breast CSCs. The mechanism by which IMP3 activates TAZ involves both mRNA stability and transcriptional regulation. IMP3 stabilizes the mRNA of an alternative WNT ligand (WNT5B) indirectly by repressing miR145-5p, which targets WNT5B, resulting in TAZ activation by alternative WNT signaling. IMP3 also facilitates the transcription of SLUG, which is necessary for TAZ nuclear localization and activation, by a mechanism that is also mediated by WNT5B. These results demonstrate that TAZ can be regulated by an mRNA-binding protein and that this regulation involves the integration of Hippo and alternative WNT-signaling pathways.**

## INTRODUCTION

IMP3 (insulin-like growth factor-2 [IGF2] mRNA-binding protein 3) is a member of a family of IGF2 mRNA-binding proteins that function in RNA stabilization, trafficking, and localization (Nielsen et al., 1999). This protein has attracted considerable interest because it exhibits the properties of an oncofetal protein, and its expression correlates with the aggressive behavior of many tumors (Degrauwe et al., 2016; Jiang et al., 2006; Walter et al., 2009; Wei et al., 2017). In breast cancer, IMP3 is associated with the highly aggressive triple-negative (TNBC) subtype (Walter et al., 2009). The challenge is to identify specific proteins and functions that are regulated by IMP3 and to establish the contribution of IMP3 to the distinguishing features of TNBC. In this direction, we implicated IMP3 in the function of breast cancer stem cells (CSCs) (Samanta et al., 2016), which is relevant because TNBCs contain a much higher frequency of CSCs than other breast cancer subtypes and this population of cells is thought to be responsible for their aggressive behavior (Pece et al., 2010). These findings are consistent with other studies on the contribution of IMP3 to CSCs (Degrauwe et al., 2016).

IMP3 has the potential to impact the expression of a multitude of proteins, a consideration that has been substantiated by individual nucleotide resolution UV crosslinking and immunoprecipitation (iCLIP) studies (Conway et al., 2016; Palanichamy et al., 2016). Based on this fact, there is a need to identify specific proteins that are regulated by IMP3, which are also important for the biology of TNBC. As an approach to this problem, we compared the mRNA expression profile of TNBC cells to the same cells that had been depleted of IMP3. The results obtained revealed that the expression of genes known to be regulated by the Hippo effectors YAP and TAZ is influenced by IMP3. This observation piqued our interest because TAZ, in particular, has been implicated in TNBC and the function of breast CSCs (Cordenonsi et al., 2011; Park et al., 2015). For this reason, we investigated the hypothesis that IMP3 facilitates TAZ activation and pursued the mechanism involved.

## RESULTS

### Causal Relationship between IMP3 and TAZ in Breast Cancer

To discover novel IMP3 targets that impact the aggressive behavior of TNBC, we performed RNA sequencing analysis using a TNBC cell line (SUM-1315) that had been transfected with either a control small hairpin RNA (shRNA) or shRNAs specific for IMP3 (see Tables S1 and S2 for a summary of results). Analysis of the sequencing data using gene set enrichment analysis (GSEA) revealed a causal link between IMP3 and the expression of established TAZ and YAP target genes (CTGF, CYR61, and DKK1) (Piccolo et al., 2014; Yu and Guan, 2013) (Figure S1A), which we verified by qPCR (Figure 1A). To gain additional insight into the relationship between IMP3 and YAP/TAZ in breast cancer, we analyzed gene expression profiles of 2,509 patients using cBioPortal (Cerami et al., 2012; Gao et al., 2013). A positive

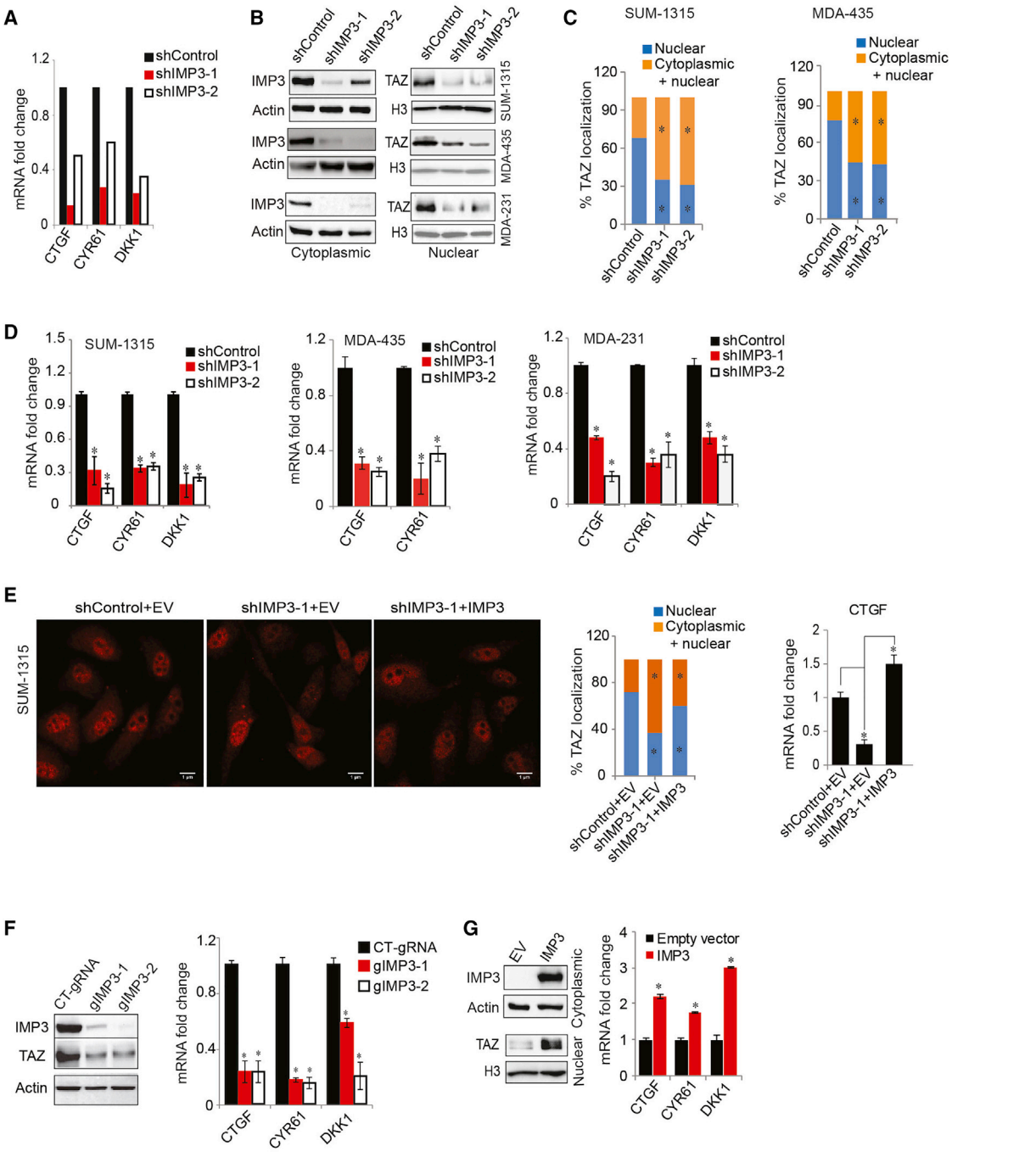


**Figure 1. Causal Relationship of IMP3 and TAZ in TNBC**

(A) RNA sequencing result showing decreased expression of CTGF, CYR61, and DKK1 upon IMP3 depletion.

(B–D) Control and IMP3-depleted SUM-1315, MDA-435, and MDA-231 cells were (B) fractionated and blotted for IMP3 (cytoplasmic) and TAZ (nuclear) (actin and histone H3 were used as loading controls for cytoplasmic and nuclear proteins, respectively); (C) assessed for TAZ localization by immunofluorescence (the bar graphs show the quantification of TAZ localization in either the nucleus only or in both cytoplasm and nucleus); and (D) assayed for TAZ target gene expression by qPCR.

(E) Control and IMP3-depleted SUM-1315 cells were transfected with an empty vector (EV) or IMP3-expressing construct that is resistant to shIMP3-1 and stained for TAZ by immunofluorescence, and TAZ localization was quantified. Total RNA isolated from the same cells was used to quantify CTGF mRNA by qPCR (right bar graph). Scale bar, 1 μm.

*(legend continued on next page)*

correlation between IMP3 and TAZ mRNA expression was observed, and their expression was enriched in basal-like and claudin-low subtypes of breast cancers, the majority of which are TNBCs (Figures S1B and S1C) (Badve et al., 2011; Prat et al., 2010). We substantiated this result by demonstrating that IMP3 and TAZ co-localize in TNBC (Figure S1D). In contrast, YAP and IMP3 mRNA expression did not correlate significantly, and the expression of YAP is distributed across breast cancer subtypes (Figures S1B and S1C). Moreover, nuclear localization of TAZ is associated with TNBC (Díaz-Martín et al., 2015), but YAP nuclear localization does not correlate with any specific subtype (Vlug et al., 2013; Yuan et al., 2008). For these reasons, we focused our efforts on IMP3 and TAZ.

The hypothesis emerged from the foregoing data that IMP3 contributes to TAZ activation in TNBC. Before testing, we excluded the possibility that IMP3 affects TAZ indirectly by influencing cell proliferation (Figure S1E). Since nuclear localization is an indicator of TAZ activation, we compared TAZ localization in control and IMP3-depleted cells using both sub-cellular fractionation and immunofluorescence. IMP3 depletion caused a significant decrease in nuclear TAZ localization and a concomitant increase in its cytoplasmic localization (Figures 1B and 1C). Also, IMP3 depletion decreased the expression of TAZ target genes significantly (Figures 1D and S1F).

Subsequently, we strengthened our conclusion that IMP3 facilitates TAZ activation. To control for the specificity of IMP3 depletion, we expressed IMP3 in IMP3-depleted cells using a construct that is resistant to shRNA, and we observed that this construct was able to rescue TAZ nuclear localization, as well as target gene expression (Figure 1E). CRISPR-mediated IMP3 depletion in SUM-1315 cells also reduced TAZ expression and the expression of TAZ target genes (Figure 1F). We also made use of SKBR3 cells, a non-TNBC cell line, because they do not express IMP3 and express low levels of TAZ (Figure 1G). Exogenous expression of IMP3 in these cells increased nuclear TAZ expression, as well as TAZ target genes (Figure 1G).

## IMP3 Activation of TAZ Is Mediated by WNT5B

In the search for a mechanism by which IMP3 activates TAZ, a possibility was that IMP3 increases TAZ mRNA stability. We observed, however, that IMP3 depletion affected neither TAZ mRNA expression nor its stability (Figure S2A). For this reason, we were intrigued by our RNA sequencing data that the expression of WNT5B, an alternative WNT ligand (Park et al., 2015), was diminished upon IMP3 depletion, because alternative Wnt signaling has been implicated in TAZ activation (Park et al., 2015).

The findings on WNT5B led us to hypothesize that the contribution of IMP3 to TAZ activation is mediated by WNT5B and that IMP3 regulates the expression of this non-canonical WNT ligand directly. In pursuit of this hypothesis, we found that IMP3 depletion in TNBC cell lines decreased WNT5B protein and mRNA expression (Figures 2A and S2B) and exogenous expression of IMP3 in SKBR3 cells increased WNT5B (Figure 2B), verifying our RNA sequencing data. Moreover, depletion of WNT5B reduced nuclear TAZ (Figure S2C), and its expression in IMP3-depleted cells rescued TAZ target gene expression and nuclear TAZ localization and it increased cytoplasmic TAZ (Figures 2C and S2D). Importantly, we observed that IMP3 stabilizes WNT5B mRNA (Figure S2E), providing a mechanism for how IMP3 influences WNT5B expression.

We presumed that IMP3 binds directly to WNT5B mRNA, but analysis of three independent published databases of IMP3-bound mRNAs did not support this idea (Conway et al., 2016; Ennajdaoui et al., 2016; Palanichamy et al., 2016). We noticed, however, that miR145-5p is elevated upon IMP3 depletion (Figure 2D), which is relevant because this miR targets WNT5B (Vlachos et al., 2015) and it is suppressed in TNBC (Sugita et al., 2016). These observations suggested that IMP3 stabilizes WNT5B mRNA by suppressing miR145-5p. Indeed, expression of an anti-miR145-5p oligonucleotide in IMP3-depleted SUM-1315 cells increased WNT5B mRNA, as well as TAZ target gene expression (Figure 2E).

The mechanism by which alternative Wnt signaling activates TAZ involves Rho GTPase activation and the consequent inhibition of large tumor suppressor kinase (LATS) activity (Park et al., 2015; Yu et al., 2012). This is significant because LATS directly phosphorylates TAZ at the serine 89 position and inhibits its nuclear localization and ability to regulate target gene expression (Park et al., 2015). In support of our hypothesis that IMP3 activates TAZ by WNT5B signaling, we observed that LPA, a Rho activator, rescued TAZ target gene expression in IMP3-depleted cells (Figure 2F). Moreover, depletion of either IMP3 or WNT5B increased LATS activity, as measured by phospho-LATS1 (Thr1079) and phospho-TAZ (Ser89), but it did not impact LATS1 expression (Figure 2G).

A critical issue is whether IMP3 stabilization of WNT5B mRNA and consequent TAZ activation are relevant to the function of this RNA-binding protein. Previously, we reported that IMP3 contributes to mammosphere formation (Samanta et al., 2016), which is also dependent on TAZ activation (Cordenonsi et al., 2011). For this reason, we assessed whether WNT5B contributed to mammosphere formation and whether it could rescue the ability of IMP3-depleted cells to form mammospheres. Indeed, we found that depletion of WNT5B decreased the mammosphere-forming ability of SUM-1315 cells (Figure 2H, left bar graph) and expression of WNT5B in IMP3-depleted cells rescued mammosphere formation (Figure 2H, right bar graph). Moreover, shRNA-mediated TAZ depletion decreased mammosphere formation (Figure 2I) and exogenous expression of a constitutively active TAZ (4SA-TAZ) (Lei et al., 2008) in either IMP3-depleted or

(F) IMP3 expression was depleted using IMP3-specific guide RNAs (gIMP3-1 and gIMP3-2) in SUM-1315 cells and assayed for expression of TAZ (immunoblots) and its target genes (qPCR). A non-targeting gRNA (CT-gRNA) was used as the control.

(G) SKBR3 cells were transfected with an empty vector or a construct expressing IMP3 and fractionated and blotted for IMP3 (cytoplasmic) and TAZ (nuclear). Total RNA extracted from the same cells was used to quantify TAZ target genes using qPCR. $p \leq 0.05$.

Relevant data are shown as ± SE.

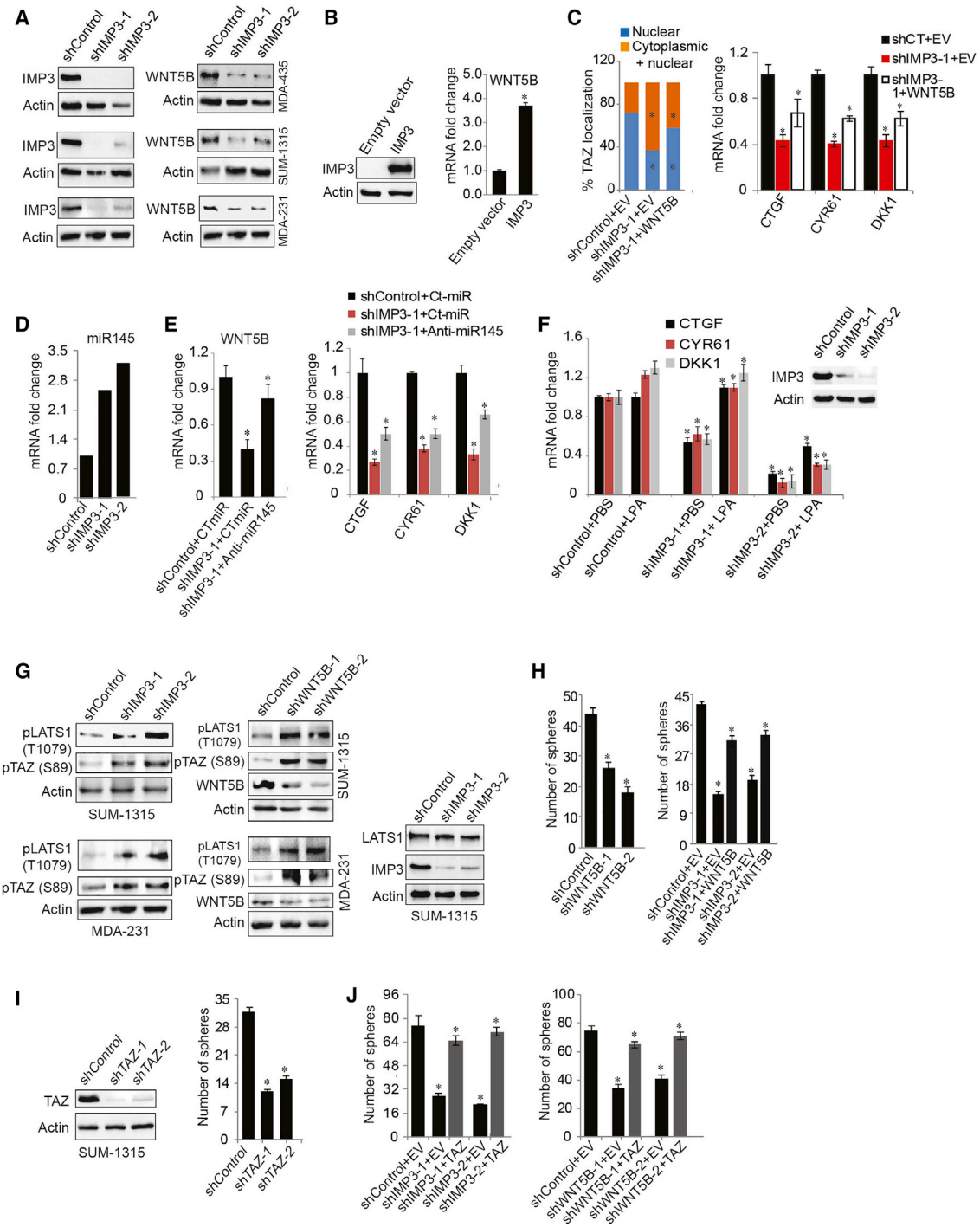


**Figure 2. IMP3 Activation of TAZ Is Mediated by WNT5B**

(A) Control and IMP3-depleted SUM-1315, MDA-435, and MDA-231 cells were blotted for WNT5B protein.

(B) SKBR3 cells were transiently transfected (48 hr) with an empty vector or IMP3-expressing construct (left immunoblot), and WNT5B mRNA was quantified by qPCR using total RNA isolated from these cells (right bar graph).

(C) Control and IMP3-depleted SUM-1315 cells were transiently transfected with an empty vector (EV) or WNT5B-expressing construct for 48 hr. TAZ localization was quantified in these cells by immunofluorescence (left bar graph). Total RNA was extracted and used to quantify the genes indicated in the right bar graph by qPCR.

(D) RNA sequencing result showing increased expression of miR-145-5p upon IMP3 depletion.

*(legend continued on next page)*

WNT5B-depleted cells increased mammosphere formation (Figure 2J). Also, the expression of WNT5B, TAZ, and its target genes is elevated in breast CSCs compared to non-CSCs (Al-Hajj et al., 2003) (Figure S2F).

To exclude the possibility that IMP3 contributes to canonical WNT signaling, we noted that the canonical WNT3A ligand is expressed at low levels in TNBC compared to other breast cancer subtypes (Figure S2G). Also, we discovered that β-catenin is primarily non-nuclear in TNBC cell lines and tumor specimens and localized in cell membranes (Figure S2H). Moreover, IMP3 depletion did not impact β-catenin localization (data not shown). There is also evidence that β-catenin is expressed at low levels in TNBC (Shen et al., 2016).

### Role of SLUG in IMP3 and WNT5B-Mediated TAZ Activation

Previously, we reported that one mechanism by which IMP3 contributes to the aggressive behavior of TNBC and breast CSCs is to regulate SLUG (Samanta et al., 2016). Moreover, analysis of the cBioPortal database revealed that SLUG is expressed preferentially in TNBC and claudin-low tumors and that it correlates with TAZ (Figure 3A). These findings are relevant because SLUG has been shown to stabilize TAZ protein and maintain its nuclear localization (Tang et al., 2016). For this reason, we investigated a possible relationship between IMP3 regulation of WNT5B and SLUG. Initially, we found that SLUG depletion in TNBC cell lines reduced nuclear TAZ and increased TAZ cytoplasmic localization (Figures 3B and S3A) and it decreased the expression of TAZ target genes (Figure 3C). Also, exogenous expression of SLUG in SKBR3 cells increased both nuclear TAZ and TAZ target genes (Figure 3D). More definitive evidence was obtained by rescuing SLUG expression in IMP3-depleted cells and observing a significant increase in TAZ target genes (Figure 3E) and nuclear TAZ (Figure S3B). Interestingly, although SLUG depletion increased TAZ phosphorylation, LATS1 phosphorylation remained unchanged (Figure 3F). This observation verifies the report that SLUG promotes TAZ nuclear retention without affecting LATS kinase activity (Tang et al., 2016). Moreover, treatment of SLUG-depleted cells with the Rho activator LPA did not rescue TAZ target gene expression (Figure S3C), in agreement with the report that SLUG activation of TAZ is independent of LATS kinase activity (Tang et al., 2016).

Although IMP3 regulates SLUG mRNA expression, it does not impact the stability of SLUG mRNA (Figure S4A), suggesting that it may contribute to the regulation of SLUG transcription. Transfection of a luciferase reporter construct containing a 4-kb SLUG promoter in control and IMP3-depleted cells revealed that IMP3 depletion decreased luciferase activity significantly (Figure 4A). In an effort to integrate WNT5B into this mechanism, we observed that WNT5B depletion reduced SLUG expression significantly (Figure 4B), as well as TAZ target gene expression (Figure 4C). In contrast, modulating SLUG expression had no effect on WNT5B expression, indicating that SLUG functions downstream of WNT5B (Figure S4B). Importantly, expression of WNT5B in IMP3-depleted cells rescued SLUG mRNA (Figure 4D), as well as activity of the SLUG reporter construct (Figure 4E). These data are strengthened by a positive correlation between WNT5B and SLUG mRNA expression in patients (Figure 4F).

## DISCUSSION

This study contributes significantly to our understanding of how IMP3 impacts the behavior of breast cancer cells, especially cells from TNBCs. The fact that IMP3 is expressed preferentially in TNBC among all the subtypes of breast cancer (Walter et al., 2009) (Figure S1B) has suggested a causal role for this RNA-binding protein in the aggressive behavior of these tumors, which are characterized by a high frequency of CSCs (Pece et al., 2010). Our implication of IMP3 in TAZ activation establishes this causal link because TAZ itself is expressed preferentially in TNBC and it is important for breast CSCs, as well as the aggressive behavior of poorly differentiated tumors (Cordenonsi et al., 2011). Moreover, our demonstration that the mechanism involves IMP3 regulation of a non-canonical WNT ligand (WNT5B) reveals the importance of this signaling pathway and its coordination with Hippo signaling in TNBC.

Although the importance of TAZ in breast and other cancers has been affirmed (Zanconato et al., 2016), the mechanisms that regulate its activation are less well understood. Our implication of IMP3 in TAZ activation provides one mechanism for TNBC. Moreover, we discovered that this mechanism involves the ability of IMP3 to regulate the stability of WNT5B mRNA indirectly by repressing the expression of an miR that targets WNT5B, enabling alternative WNT signaling. This observation may relate to the interesting finding that IMP3 ribonucleoprotein granules can function as safehouses that protect against miR-mediated decay of target genes (Jønson et al., 2014). Our

(E) Control and IMP3-depleted SUM-1315 cells were transfected with either a control or anti-miR-145 oligonucleotide (20 nM) for 48 hr, and expression of WNT5B and TAZ target genes mRNA was quantified by qPCR.
(F) Total RNA extracted from LPA- (1 μM, 2 hr) treated control and IMP3-depleted SUM-1315 cells was used to quantify TAZ target genes by qPCR. Blot inset shows IMP3 depletion.
(G) Total cell extracts from control, IMP3-depleted, and WNT5B-depleted SUM-1315 and MDA-231 cells were blotted for pLATS1 (T1079), pTAZ (S89), and WNT5B. pTAZ (S89) blots were obtained using a pYAP(S127) antibody that detects both pTAZ (S89) and pYAP.
(H) Control and WNT5B-depleted (shWNT5B-1 and shWNT5B-2) SUM-1315 cells were grown as mammospheres for 7 days, and the number of spheres was quantified (left). Control and IMP3-depleted SUM-1315 cells were transiently transfected with an empty vector (EV) or a construct expressing WNT5B ligand, grown as mammospheres for 7 days, and the number of spheres was quantified (right).
(I) Total extracts from control and TAZ-depleted (shTAZ-1 and shTAZ-2) SUM-1315 cells were blotted for TAZ (left blot). The same cells were grown as mammospheres for 7 days and quantified (right graph).
(J) Control, IMP3, and WNT5B-depleted SUM-1315 cells were transfected with an empty vector or a vector expressing 4SA-TAZ, grown as mammospheres for 7 days, and quantified. $p \leq 0.05$.
Relevant data are shown as ± SE.

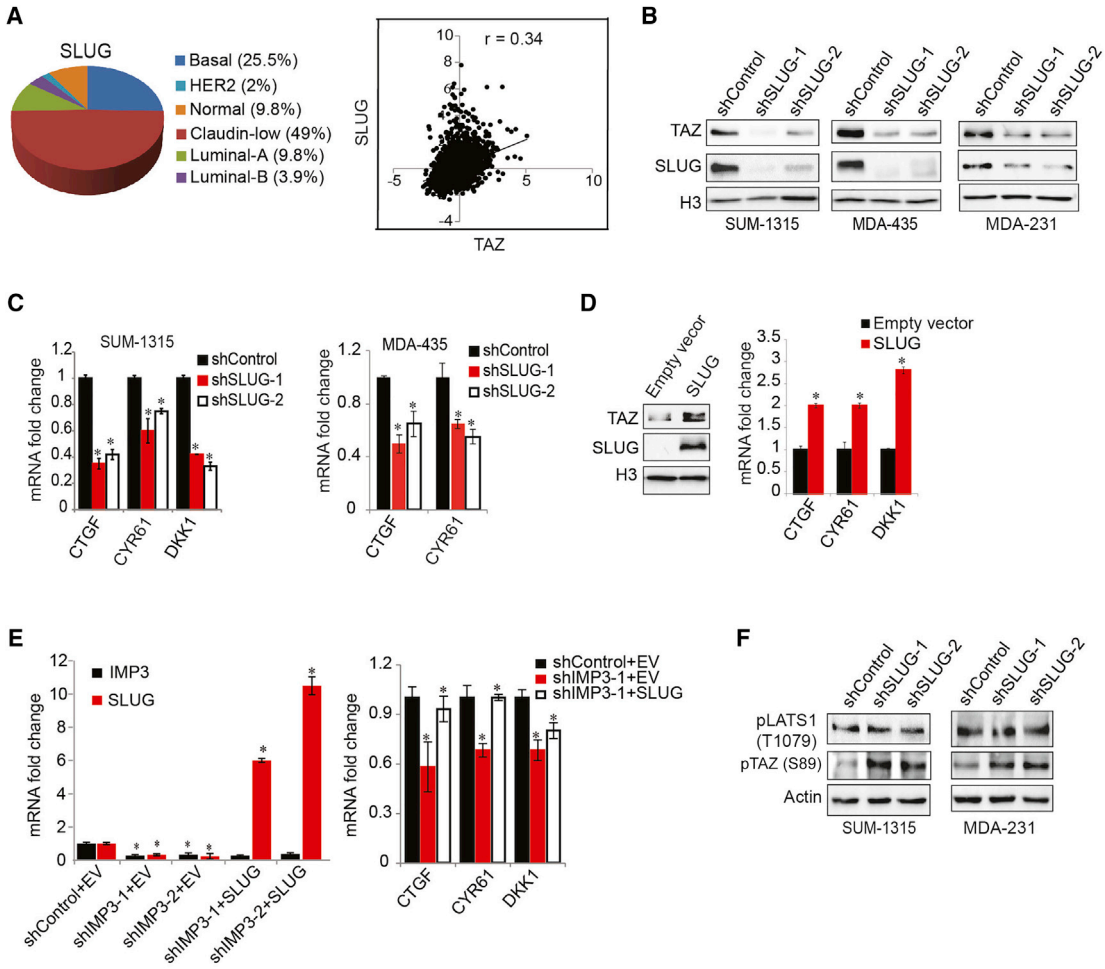


**Figure 3. SLUG Is Necessary for IMP3 Activation of TAZ**

(A) Pie chart showing SLUG mRNA expression in breast cancer subtypes (PAM50 classification, cBioPortal). SLUG and TAZ expression was correlated using the same database (right graph).

(B and C) SLUG expression was depleted using shRNAs (shSLUG-1 and shSLUG-2) in SUM-1315, MDA-435, and MDA-231 cells, and nuclear fractions were blotted for SLUG and TAZ (B). The same cells were used to quantify TAZ target genes using qPCR (C).

(D) SKBR3 cells were transfected with an empty vector or a construct expressing SLUG, and nuclear fractions were blotted for SLUG and TAZ. Total RNA extracted from the same cells was used to quantify TAZ target genes by qPCR.

(E) Control and IMP3-depleted SUM-1315 cells were transiently transfected with an empty vector (EV) or SLUG-expressing construct. Total RNA was extracted and used to quantify TAZ target genes by qPCR.

(F) Total cell extracts from control and SLUG-depleted SUM-1315 and MDA-231 cells were blotted for pTAZ (S89) and LATS1 (T1079). $p \leq 0.05$.

Relevant data are shown as ± SE.

findings are consistent with the observations that WNT5B expression is enriched in TNBC compared to other WNT ligands (Figure S2G) and that IMP3 is expressed specifically in TNBC (Walter et al., 2009). Surprisingly, however, the expression of WNT5A, another alternative WNT ligand, is very low in TNBC and appears to be independent of IMP3 regulation. This observation is intriguing because WNT5A has been shown to enhance the growth of mammary stem/progenitor cells (Kessenbrock et al., 2017). In contrast, WNT5B represses the growth of these cells (Kessenbrock et al., 2017), suggesting that the function and expression of these alternative WNT ligands differ in mammary gland biology and cancer.

Another important conclusion from our study is that IMP3 influences TAZ activation at multiple levels: WNT5B mRNA stability and SLUG transcription. Previously, we had reported that IMP3 regulation of SLUG contributes to the behavior of TNBC cells, but the mechanism involved escaped us and we were unable to demonstrate that IMP3 affected SLUG mRNA stability (Samanta et al., 2016). The data obtained here indicate that IMP3 regulates SLUG expression at the transcriptional level and that this regulation is mediated by WNT5B by a mechanism that remains to be determined. We also demonstrate that SLUG is necessary for TAZ nuclear localization and activation, confirming a previous study on osteogenesis (Tang et al., 2016). Similar to

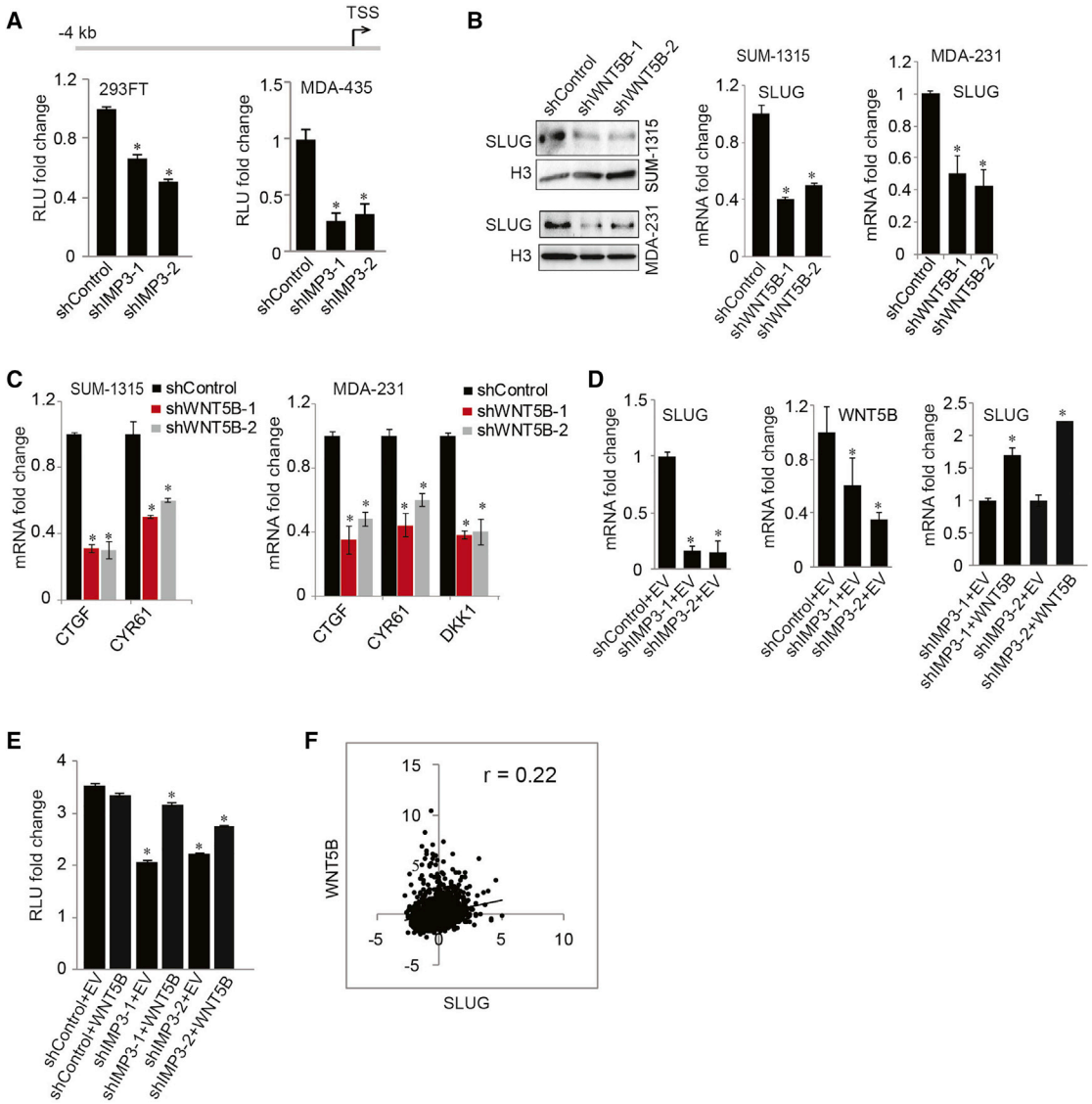


**Figure 4. WNT5B Mediates SLUG Transcription**

(A) Control and IMP3-depleted HEK293FT and MDA-435 cells were transfected with a reporter construct bearing a 4-kb SLUG promoter upstream of firefly luciferase, and they were assayed for luciferase activity (RLU) 24 hr post-transfection.

(B and C) Nuclear extracts from control and WNT5B-depleted SUM-1315 and MDA-231 cells were blotted for SLUG protein, and total RNA extracted from these cells was used to quantify SLUG mRNA (B) and TAZ target genes by qPCR (C).

(D) Control and IMP3-depleted MDA-435 cells (shIMP3-1 and shIMP3-2) were transiently transfected with an empty vector or WNT5B-expressing construct. Total RNA was extracted and used to quantify SLUG and WNT5B mRNA by qPCR.

(E) Control and IMP3-depleted HEK293FT cells were transfected with an empty vector (EV) or a construct expressing WNT5B. These cells were re-transfected 24 hr later with a SLUG-luciferase reporter construct and assayed for luciferase activity after another 24 hr.

(F) Expression of WNT5B and SLUG mRNA was correlated using cBioportal. The correlation coefficient (r) was estimated using Pearson's correlation. *$p \leq 0.05$.

Relevant data are shown as ± SE.

IMP3 and WNT5B, SLUG is expressed preferentially in TNBC, and it has been implicated in the genesis of these tumors (Guo et al., 2012; Zhou et al., 2016). For this reason, mechanisms that regulate its expression are critically important. There is evidence, for example, that the SIRT deacetylase stabilizes SLUG protein in this breast cancer subtype (Zhou et al., 2016). Our findings suggest that SLUG expression can be regulated by multiple mechanisms in TNBC, including transcription. Moreover, the possibility that WNT5B contributes to the mechanism of SLUG transcription suggests a novel function for this alternative WNT ligand that may be distinct from the pathway by which it activates TAZ by inhibiting LATS1/2 phosphorylation (Park et al., 2015).

## EXPERIMENTAL PROCEDURES

### RNA Sequencing Analysis

RNA sequencing analysis was performed using total RNA extracted from control (shControl) and IMP3-depleted SUM-1315 cells. See the Supplemental Experimental Procedures for details.

### Biochemical Assays

Immunoblotting of whole-cell extracts, as well as cytoplasmic and nuclear fractions, and qPCR were performed as described previously (Samanta et al., 2016). Primers used for qPCR are listed in Table S3. Mammosphere assays were performed as described previously (Samanta et al., 2016). For the reporter assay, control or IMP3-depleted HEK293T cells were transfected with a firefly luciferase reporter vector containing the SLUG promoter (4 kb) (Chakrabarti et al., 2012) and assayed after 24 hr. A construct expressing renilla luciferase was used as the transfection control. The relative light unit (RLU) value was calculated as the ratio of firefly luciferase to renilla luciferase activity (normalized luciferase activity). To measure mRNA stability, control and IMP3-depleted SUM-1315 cells were treated with actinomycin-D (5 μg/mL). Total RNA was extracted and the expression of specific mRNAs was quantified by qPCR.

### Immunofluorescence Staining

Immunofluorescence staining of TAZ was performed as described previously (Chang et al., 2015). The same protocol was used to stain β-catenin. Human breast tumor sections were provided by Dr. Ashraf Khan (University of Massachusetts Medical School).

### Statistical Analysis

The data are shown as the ± SE. The p values (*) were determined using a Student's t test and $p \leq 0.05$ was considered significant. For correlation studies, statistical significance was calculated by Pearson's correlation.

## DATA AND SOFTWARE AVAILABILITY

The accession number for the sequencing data reported in this paper is GEO: GSE107564.

## SUPPLEMENTAL INFORMATION

Supplemental Information includes Supplemental Experimental Procedures, four figures, and three tables and can be found with this article online at https://doi.org/10.1016/j.celrep.2018.04.113.

## ACKNOWLEDGMENTS

We thank Drs. Ashraf Khan, Yibin Kang, Junhao Mao, and Bob Veralas for providing reagents. This work was supported by NIH grants CA168464 and CA203439 (A.M.M.). A.L.E. was supported by a Ruth L. Kirschstein National Research Service Award from the NCI (F30CA206271).

## AUTHOR CONTRIBUTIONS

S.S. and A.M.M. designed experiments and wrote the manuscript. S.G. and A.L.E. performed specific experiments. J.J.A. provided technical support. J.O., J.Y., and L.J.Z. performed the bioinformatics.

## DECLARATION OF INTERESTS

The authors declare no competing interests.

Received: December 1, 2017
Revised: March 16, 2018
Accepted: April 26, 2018
Published: May 29, 2018

## REFERENCES

Al-Hajj, M., Wicha, M.S., Benito-Hernandez, A., Morrison, S.J., and Clarke, M.F. (2003). Prospective identification of tumorigenic breast cancer cells. Proc. Natl. Acad. Sci. USA *100*, 3983–3988.

Badve, S., Dabbs, D.J., Schnitt, S.J., Baehner, F.L., Decker, T., Eusebi, V., Fox, S.B., Ichihara, S., Jacquemier, J., Lakhani, S.R., et al. (2011). Basal-like and triple-negative breast cancers: a critical review with an emphasis on the implications for pathologists and oncologists. Mod. Pathol. *24*, 157–167.

Cerami, E., Gao, J., Dogrusoz, U., Gross, B.E., Sumer, S.O., Aksoy, B.A., Jacobsen, A., Byrne, C.J., Heuer, M.L., Larsson, E., et al. (2012). The cBio cancer genomics portal: an open platform for exploring multidimensional cancer genomics data. Cancer Discov. *2*, 401–404.

Chakrabarti, R., Hwang, J., Andres Blanco, M., Wei, Y., Lukačišin, M., Romano, R.A., Smalley, K., Liu, S., Yang, Q., Ibrahim, T., et al. (2012). Elf5 inhibits the epithelial-mesenchymal transition in mammary gland development and breast cancer metastasis by transcriptionally repressing Snail2. Nat. Cell Biol. *14*, 1212–1222.

Chang, C., Goel, H.L., Gao, H., Pursell, B., Shultz, L.D., Greiner, D.L., Ingerpuu, S., Patarroyo, M., Cao, S., Lim, E., et al. (2015). A laminin 511 matrix is regulated by TAZ and functions as the ligand for the α6Bβ1 integrin to sustain breast cancer stem cells. Genes Dev. *29*, 1–6.

Conway, A.E., Van Nostrand, E.L., Pratt, G.A., Aigner, S., Wilbert, M.L., Sundararaman, B., Freese, P., Lambert, N.J., Sathe, S., Liang, T.Y., et al. (2016). Enhanced CLIP Uncovers IMP Protein-RNA Targets in Human Pluripotent Stem Cells Important for Cell Adhesion and Survival. Cell Rep. *15*, 666–679.

Cordenonsi, M., Zanconato, F., Azzolin, L., Forcato, M., Rosato, A., Frasson, C., Inui, M., Montagner, M., Parenti, A.R., Poletti, A., et al. (2011). The Hippo transducer TAZ confers cancer stem cell-related traits on breast cancer cells. Cell *147*, 759–772.

Degrauwe, N., Suvà, M.L., Janiszewska, M., Riggi, N., and Stamenkovic, I. (2016). IMPs: an RNA-binding protein family that provides a link between stem cell maintenance in normal development and cancer. Genes Dev. *30*, 2459–2474.

Díaz-Martín, J., López-García, M.A., Romero-Pérez, L., Atienza-Amores, M.R., Pecero, M.L., Castilla, M.A., Biscuola, M., Santón, A., and Palacios, J. (2015). Nuclear TAZ expression associates with the triple-negative phenotype in breast cancer. Endocr. Relat. Cancer *22*, 443–454.

Ennajdaoui, H., Howard, J.M., Sterne-Weiler, T., Jahanbani, F., Coyne, D.J., Uren, P.J., Dargyte, M., Katzman, S., Draper, J.M., Wallace, A., et al. (2016). IGF2BP3 Modulates the Interaction of Invasion-Associated Transcripts with RISC. Cell Rep. *15*, 1876–1883.

Gao, J., Aksoy, B.A., Dogrusoz, U., Dresdner, G., Gross, B., Sumer, S.O., Sun, Y., Jacobsen, A., Sinha, R., Larsson, E., et al. (2013). Integrative analysis of complex cancer genomics and clinical profiles using the cBioPortal. Sci. Signal. *6*, pl1.

Guo, W., Keckesova, Z., Donaher, J.L., Shibue, T., Tischler, V., Reinhardt, F., Itzkovitz, S., Noske, A., Zürrer-Härdi, U., Bell, G., et al. (2012). Slug and Sox9 cooperatively determine the mammary stem cell state. Cell *148*, 1015–1028.

Jiang, Z., Chu, P.G., Woda, B.A., Rock, K.L., Liu, Q., Hsieh, C.C., Li, C., Chen, W., Duan, H.O., McDougal, S., and Wu, C.L. (2006). Analysis of RNA-binding protein IMP3 to predict metastasis and prognosis of renal-cell carcinoma: a retrospective study. Lancet Oncol. *7*, 556–564.

Jønson, L., Christiansen, J., Hansen, T.V., Vikeså, J., Yamamoto, Y., and Nielsen, F.C. (2014). IMP3 RNP safe houses prevent miRNA-directed HMGA2 mRNA decay in cancer and development. Cell Rep. *7*, 539–551.

Kessenbrock, K., Smith, P., Steenbeek, S.C., Pervolarakis, N., Kumar, R., Minami, Y., Goga, A., Hinck, L., and Werb, Z. (2017). Diverse regulation of mammary epithelial growth and branching morphogenesis through noncanonical Wnt signaling. Proc. Natl. Acad. Sci. USA *114*, 3121–3126.

Lei, Q.Y., Zhang, H., Zhao, B., Zha, Z.Y., Bai, F., Pei, X.H., Zhao, S., Xiong, Y., and Guan, K.L. (2008). TAZ promotes cell proliferation and epithelial-mesenchymal transition and is inhibited by the hippo pathway. Mol. Cell. Biol. *28*, 2426–2436.

Nielsen, J., Christiansen, J., Lykke-Andersen, J., Johnsen, A.H., Wewer, U.M., and Nielsen, F.C. (1999). A family of insulin-like growth factor II mRNA-binding proteins represses translation in late development. Mol. Cell. Biol. *19*, 1262–1270.

Palanichamy, J.K., Tran, T.M., Howard, J.M., Contreras, J.R., Fernando, T.R., Sterne-Weiler, T., Katzman, S., Toloue, M., Yan, W., Basso, G., et al. (2016). RNA-binding protein IGF2BP3 targeting of oncogenic transcripts promotes hematopoietic progenitor proliferation. J. Clin. Invest. *126*, 1495–1511.

Park, H.W., Kim, Y.C., Yu, B., Moroishi, T., Mo, J.S., Plouffe, S.W., Meng, Z., Lin, K.C., Yu, F.X., Alexander, C.M., et al. (2015). Alternative Wnt Signaling Activates YAP/TAZ. Cell *162*, 780–794.

Pece, S., Tosoni, D., Confalonieri, S., Mazzarol, G., Vecchi, M., Ronzoni, S., Bernard, L., Viale, G., Pelicci, P.G., and Di Fiore, P.P. (2010). Biological and molecular heterogeneity of breast cancers correlates with their cancer stem cell content. Cell *140*, 62–73.

Piccolo, S., Dupont, S., and Cordenonsi, M. (2014). The biology of YAP/TAZ: hippo signaling and beyond. Physiol. Rev. *94*, 1287–1312.

Prat, A., Parker, J.S., Karginova, O., Fan, C., Livasy, C., Herschkowitz, J.I., He, X., and Perou, C.M. (2010). Phenotypic and molecular characterization of the claudin-low intrinsic subtype of breast cancer. Breast Cancer Res. *12*, R68.

Samanta, S., Sun, H., Goel, H.L., Pursell, B., Chang, C., Khan, A., Greiner, D.L., Cao, S., Lim, E., Shultz, L.D., and Mercurio, A.M. (2016). IMP3 promotes stem-like properties in triple-negative breast cancer by regulating SLUG. Oncogene *35*, 1111–1121.

Shen, T., Zhang, K., Siegal, G.P., and Wei, S. (2016). Prognostic Value of E-Cadherin and β-Catenin in Triple-Negative Breast Cancer. Am. J. Clin. Pathol. *146*, 603–610.

Sugita, B., Gill, M., Mahajan, A., Duttargi, A., Kirolikar, S., Almeida, R., Regis, K., Oluwasanmi, O.L., Marchi, F., Marian, C., et al. (2016). Differentially expressed miRNAs in triple negative breast cancer between African-American and non-Hispanic white women. Oncotarget *7*, 79274–79291.

Tang, Y., Feinberg, T., Keller, E.T., Li, X.Y., and Weiss, S.J. (2016). Snail/Slug binding interactions with YAP/TAZ control skeletal stem cell self-renewal and differentiation. Nat. Cell Biol. *18*, 917–929.

Vlachos, I.S., Paraskevopoulou, M.D., Karagkouni, D., Georgakilas, G., Vergoulis, T., Kanellos, I., Anastasopoulos, I.L., Maniou, S., Karathanou, K., Kalfakakou, D., et al. (2015). DIANA-TarBase v7.0: indexing more than half a million experimentally supported miRNA:mRNA interactions. Nucleic Acids Res. *43*, D153–D159.

Vlug, E.J., van de Ven, R.A., Vermeulen, J.F., Bult, P., van Diest, P.J., and Derksen, P.W. (2013). Nuclear localization of the transcriptional coactivator YAP is associated with invasive lobular breast cancer. Cell Oncol. (Dordr.) *36*, 375–384.

Walter, O., Prasad, M., Lu, S., Quinlan, R.M., Edmiston, K.L., and Khan, A. (2009). IMP3 is a novel biomarker for triple negative invasive mammary carcinoma associated with a more aggressive phenotype. Hum. Pathol. *40*, 1528–1533.

Wei, Q., Zhou, H., Zhong, L., Shi, L., Liu, J., Yang, Q., and Zhao, T. (2017). IMP3 expression in biopsy specimens as a diagnostic biomarker for colorectal cancer. Hum. Pathol. *64*, 137–144.

Yu, F.X., and Guan, K.L. (2013). The Hippo pathway: regulators and regulations. Genes Dev. *27*, 355–371.

Yu, F.X., Zhao, B., Panupinthu, N., Jewell, J.L., Lian, I., Wang, L.H., Zhao, J., Yuan, H., Tumaneng, K., Li, H., et al. (2012). Regulation of the Hippo-YAP pathway by G-protein-coupled receptor signaling. Cell *150*, 780–791.

Yuan, M., Tomlinson, V., Lara, R., Holliday, D., Chelala, C., Harada, T., Gangeswaran, R., Manson-Bishop, C., Smith, P., Danovi, S.A., et al. (2008). Yes-associated protein (YAP) functions as a tumor suppressor in breast. Cell Death Differ. *15*, 1752–1759.

Zanconato, F., Cordenonsi, M., and Piccolo, S. (2016). YAP/TAZ at the Roots of Cancer. Cancer Cell *29*, 783–803.

Zhou, W., Ni, T.K., Wronski, A., Glass, B., Skibinski, A., Beck, A., and Kuperwasser, C. (2016). The SIRT2 Deacetylase Stabilizes Slug to Control Malignancy of Basal-like Breast Cancer. Cell Rep. *17*, 1302–1317.

**Cell Reports, Volume *23***

## Supplemental Information

# IMP3 Stabilization of WNT5B mRNA Facilitates TAZ Activation in Breast Cancer

**Sanjoy Samanta, Santosh Guru, Ameer L. Elaimy, John J. Amante, Jianhong Ou, Jun Yu, Lihua J. Zhu, and Arthur M. Mercurio**

# Figure S1.

**A.**

shControl vs shIMP3-1

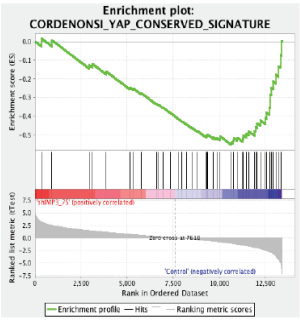


| Gene | ES |
|---|---|
| GLS | -0.5381404 |
| CRIM1 | -0.5290095 |
| PHGDH | -0.5159068 |
| LHFP | -0.513471 |
| FSCN1 | -0.5169609 |
| DAB2 | -0.5008784 |
| MDFIC | -0.4921103 |
| BIRC5 | -0.479332 |
| DUSP1 | -0.4776948 |
| MARCKS | -0.4564172 |
| ANKRD1 | -0.4363506 |
| FLNA | -0.4218539 |
| SGK1 | -0.4082211 |
| SERPINE1 | -0.3790144 |
| TGM2 | -0.3539487 |
| AMOTL2 | -0.3191373 |
| SLIT2 | -0.2828743 |
| FGF2 | -0.2476175 |
| TGFB2 | -0.2135795 |
| DLC1 | -0.1772951 |
| THBS1 | -0.1311429 |
| CYR61 | -0.0729081 |
| CTGF | 9.73E-04 |

shControl vs shIMP3-2

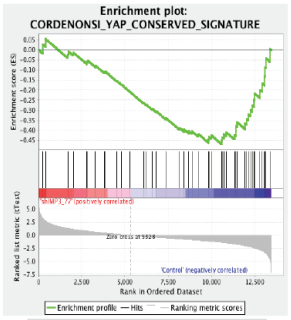


| Gene | ES |
|---|---|
| TGM2 | -0.4510482 |
| MARCKS | -0.4334959 |
| SLIT2 | -0.4196395 |
| AMOTL2 | -0.4092609 |
| GAS6 | -0.4217649 |
| HEXB | -0.4038526 |
| SERPINE1 | -0.3798229 |
| TSPAN3 | -0.3595386 |
| FSCN1 | -0.3657755 |
| PDLIM2 | -0.3440151 |
| BICC1 | -0.3216218 |
| CRIM1 | -0.2997191 |
| TGFB2 | -0.2763375 |
| CYR61 | -0.2491276 |
| PHGDH | -0.2176879 |
| DLC1 | -0.2000943 |
| TK1 | -0.1670781 |
| FGF2 | -0.1311337 |
| CTGF | -0.0872462 |
| BIRC5 | -0.0419462 |
| ETV5 | 0.0050676 |

**B.**

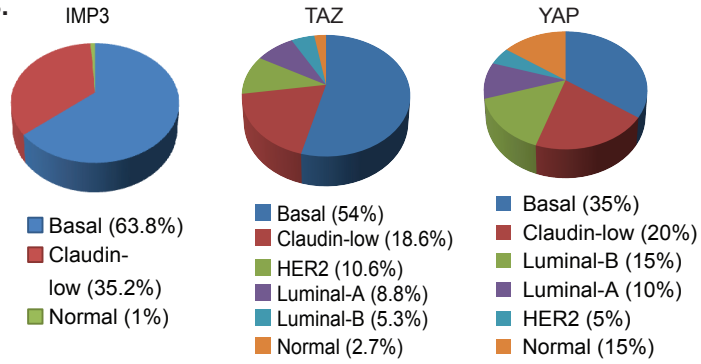


**C.**

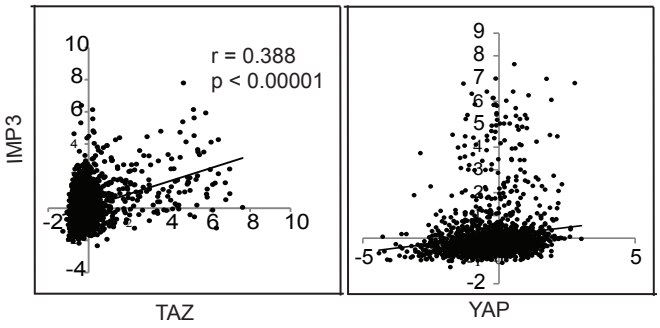


| | | p-value | Log odds ratio | Association |
|---|---|---|---|---|
| IMP3 | TAZ | <0.001 | 2.760 | Tendency towards co-occurrence |
| IMP3 | YAP | 0.335 | 0.239 | Tendency towards co-occurrence |
| TAZ | YAP | 0.557 | -0.053 | Tendency towards mutual exclisivity |

**D.**

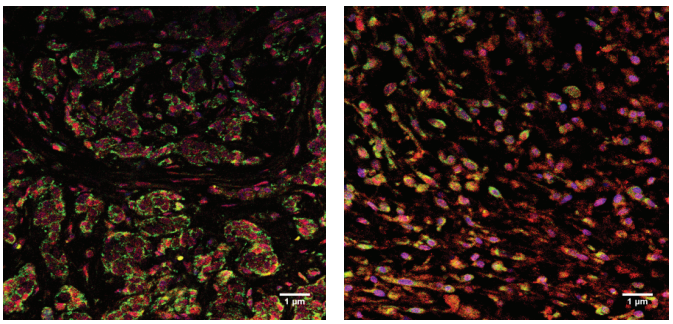

TNBC # 1 TNBC # 2

**E.**

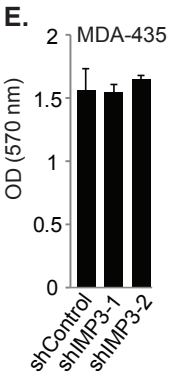


**F.**

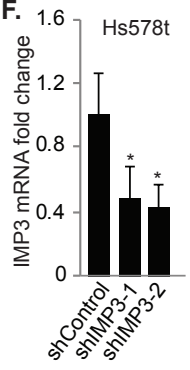


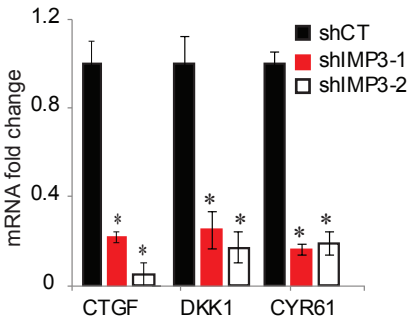

# Figure S2

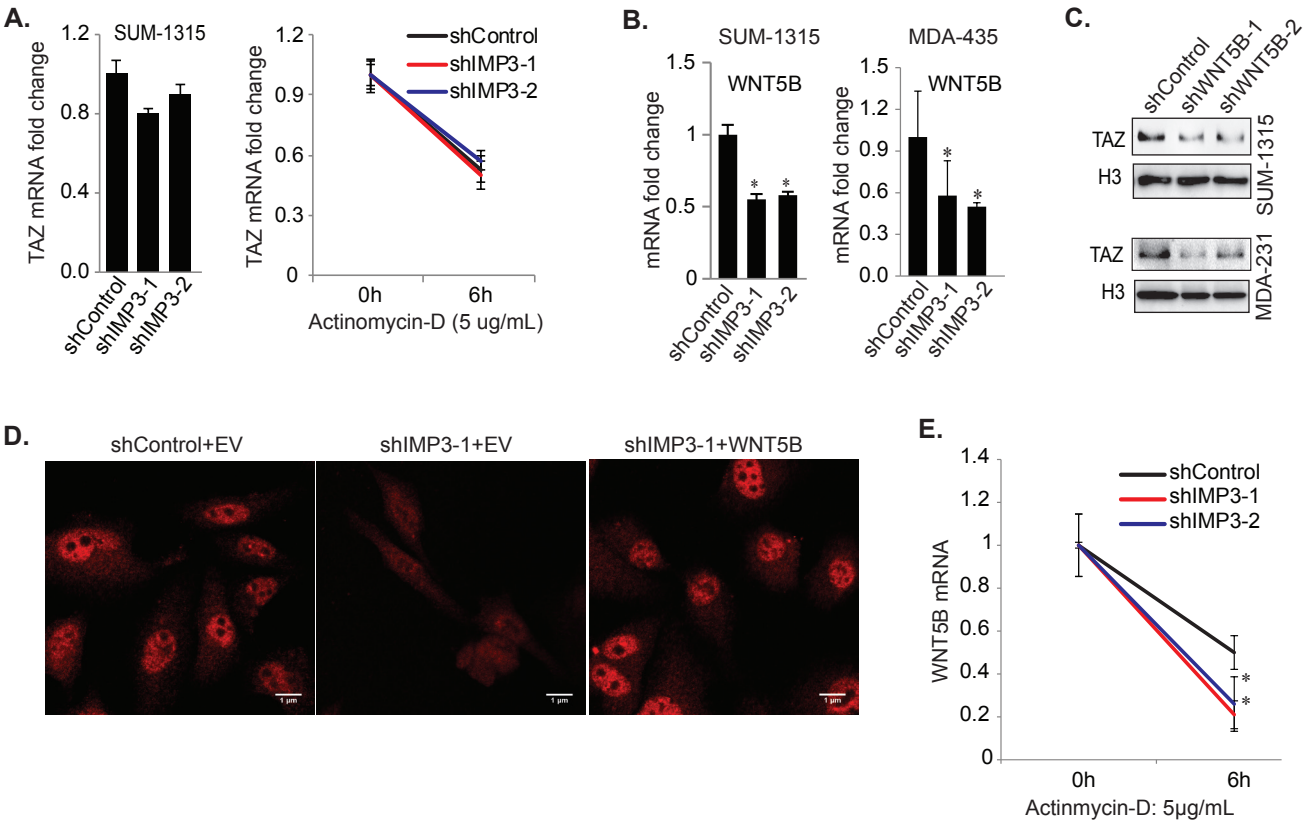


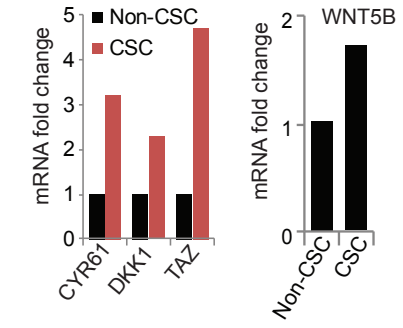


G.

cBioPortal for Cancer Genomics

| | WNT5A | WNT5B | WNT3A |
|---|---|---|---|
| Basal | 0 | 42.9 | 12.7 |
| Claudin-low | 7.5 | 21 | 9.5 |
| Luminal-A | 71.7 | 13.3 | 12.7 |
| Luminal-B | 17 | 9.5 | 27 |
| HER2 | 3.8 | 5.7 | 30.2 |
| Normal | 0 | 7.6 | 7.9 |

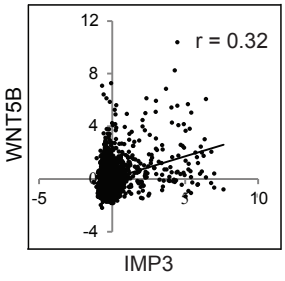


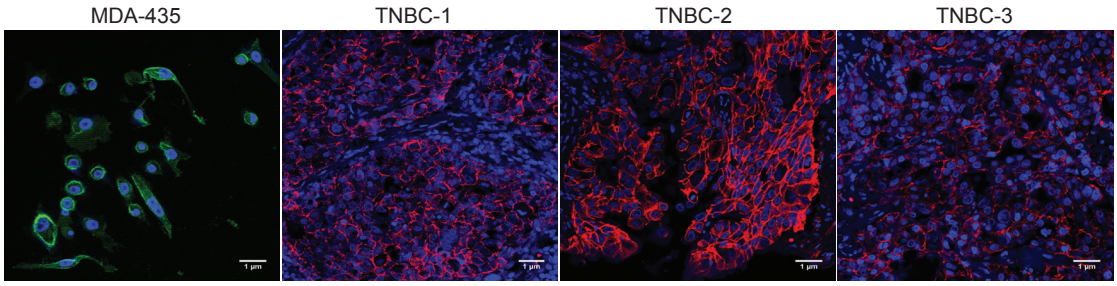

## Figure S3

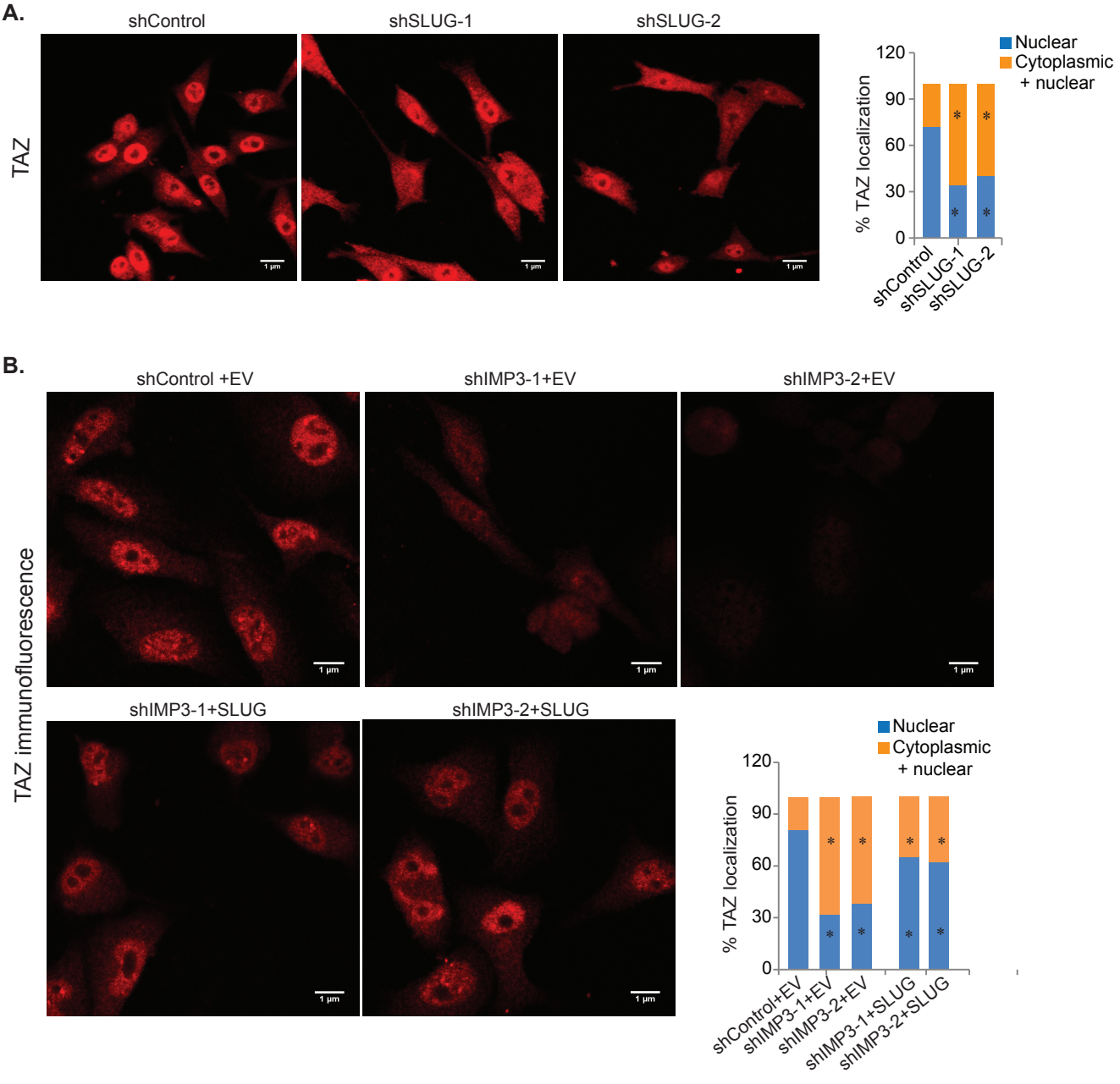
A.
shControl
shSLUG-1
shSLUG-2
TAZ
1 μm
Nuclear
Cytoplasmic
+ nuclear
% TAZ localization
120
90
60
30
0
shControl
shSLUG-1
shSLUG-2
B.
shControl +EV
shIMP3-1+EV
shIMP3-2+EV
shIMP3-1+SLUG
shIMP3-2+SLUG
TAZ immunofluorescence
Nuclear
Cytoplasmic
+ nuclear
% TAZ localization
shControl+EV
shIMP3-1+EV
shIMP3-2+EV
shIMP3-1+SLUG
shIMP3-2+SLUG
C.
mRNA fold change
1.4
1.2
1.0
0.8
0.6
0.4
0.2
0.0
CTGF
CYR61
DKK1
shControl+PBS
shControl+LPA
shSLUG-1+PBS
shSLUG-1+LPA
shSLUG-2+PBS
shSLUG-2+LPA

## Figure S4

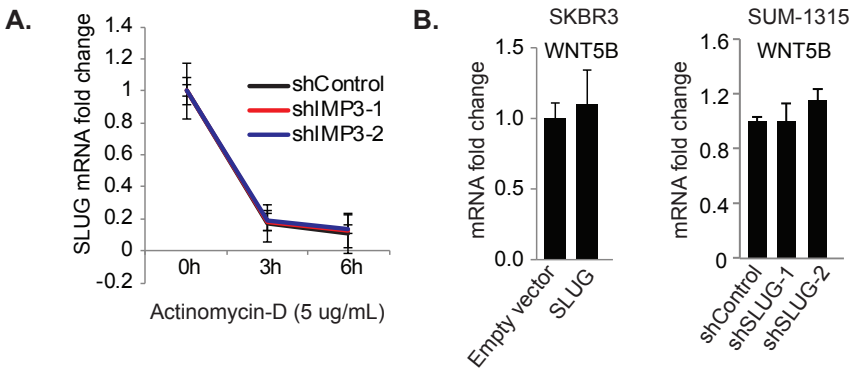
A.
SLUG mRNA fold change
1.4
1.2
1
0.8
0.6
0.4
0.2
0
-0.2
shControl
shIMP3-1
shIMP3-2
0h
3h
6h
Actinomycin-D (5 ug/mL)
B.
SKBR3
WNT5B
mRNA fold change
1.5
1.0
0.5
0.0
Empty vector
SLUG
SUM-1315
WNT5B
mRNA fold change
1.6
1.2
0.8
0.4
0
shControl
shSLUG-1
shSLUG-2

**Supplementary Figure Legends**

**Figure S1. Related to Figure 1.** (A) Gene Set Enrichment Analysis (GSEA) of RNA-sequencing data showing enrichment of conserved YAP/TAZ target genes in control (shControl) cells compared to IMP3-depleted cells. (B) Expression of IMP3, TAZ and YAP mRNA in breast cancer subtypes (PAM50 classification). Charts were generated by analyzing gene expression profiles of 2509 breast cancer patients in cBioPortal for Cancer Genomics. (C) Expression of IMP3, TAZ and YAP was correlated in a cohort of 2509 human breast tumors using cBioportal. The correlation coefficient (r) was estimated using Pearson's correlation. (D) Immunofluorescence staining on human TNBC specimens showing co-localization of IMP3 (green) and TAZ (red). Scale bar = 1µm. (E) Proliferation of control and IMP3-depleted MDA-435 cells was measured using the MTT assay. (F) Total RNA extracted from control and IMP3-depleted Hs578t cells (a TNBC cell line) were used to quantify IMP3 and TAZ targets mRNA by qPCR. $p \leq 0.05$.

**Figure S2**. **Related to Figure 2.** (A) Total RNA was extracted from control and IMP3-depleted SUM-1315 cells and used to quantify TAZ mRNA by qPCR (bar graph, left). The same cells were treated with DMSO or actinomycin-D (5 µg/mL) for 6 hours. Total RNA was isolated and used to quantify TAZ mRNA by qPCR (line graph, right) (B) Total RNA extracted from control and IMP3-depleted SUM-1315 and MDA-435 cells were used to quantify WNT5B mRNA by qPCR. (C) Nuclear extracts from control and WNT5B-depleted SUM-1315 and MDA-231 cells were blotted for TAZ. (D) Immunofluorescence staining of TAZ (red) in control (shControl) and IMP3-depleted SUM-1315 cells (shIMP3-1) that had been transiently transfected with an empty vector (EV) or a vector expressing WNT5B for 48 hours. (E) WNT5B mRNA was quantified using total RNA extracted from control and IMP3-depleted SUM-1315 cells that had been treated with DMSO or actinomycin-D (5 µg/mL) for 6 hours. (F) Expression of TAZ target genes and WNT5B mRNA

was analyzed in the breast cancer stem cells ($CD44^+CD24^-ESA^+$) and bulk populations of breast tumor cells using a published database (GEO accession no. **GSE6883**). Gene expression was analyzed in GEO2R. (G) Expression of WNT5A, WNT5B and WNT3A in breast cancer subtypes (PAM50) from cBioPortal (left chart); IMP3 and WNT5B expression was correlated in patients using cBioPortal (right plot). (H) Immunofluorescence staining of β-catenin in MDA-435 cell line (left, green) and three TNBC specimens (red). Nuclei were stained with DAPI (blue). Scale bar = 1μm.

**Figure S3**. **Related to Figure 3.** (A) Immunofluorescence staining of TAZ in control and SLUG-depleted SUM-1315 cells. Scale bar = 1μm. The graphs show the quantification of TAZ localization in either the nucleus only or in both cytoplasm and nucleus. (B) Immunofluorescence staining of TAZ (red) in control (shControl) and IMP3-depleted SUM-1315 cells (shIMP3-1 & shIMP3-2) that had been transiently transfected with an empty vector (EV) or a vector expressing SLUG for 48 hours. Scale bar = 1μm. The graphs show the quantification of TAZ localization. (C) Total RNA extracted from vehicle (phosphate-buffered saline) or LPA (1μm, 2h) treated control (shControl) and SLUG-depleted SUM-1315 cells was used to quantify TAZ target genes by qPCR. $p \leq 0.05$.

**Figure S4. Related to Figure 4.** (A) Control and IMP3-depleted SUM-1315 cells were treated with DMSO or actinomycin-D (5 μg/mL) for indicated time periods and SLUG mRNA was quantified by qPCR. (B) SKBR3 cells were transfected with an empty vector or a SLUG-expressing construct for 48h and WNT5B mRNA was quantified by qPCR (left). Right graph shows WNT5B mRNA quantification in SLUG-depleted SUM-1315 cells. $p \leq 0.05$.

**Supplemental Experimental Procedures**

**Reagents:** shRNAs specific for GFP (RHS4459), IMP3 (TRCN0000074675, TRCN0000074677), SLUG (TRCN0000015389, TRCN0000015390) were obtained from Open Biosystems (Rockford, IL, USA). shRNAs targeting WNT5B (TRCN0000437705, TRCN0000123197) were obtained from Sigma (St. Louis, MO, USA). TAZ specific shRNAs were provided by Dr. Junhao Mao (University of Massachusetts Medical School, Worcester, MA, USA). Antibodies for IMP3 (RN009P) and SLUG (L40C6) were purchased from MBL International (Woburn, MA, USA) and Cell Signaling (Danvers, MA, USA), respectively. TAZ (H-70), β-catenin (E5) and WNT5B (G-4) specific antibodies were obtained from Santa Cruz Biotechnology (Dallas, Texas, USA). Histone-H3, LATS1, pLATS1(T1079) and pYAP(S127) were purchased from Cell Signaling (Danvers, MA, USA) respectively. Beta-actin antibody was purchased from Sigma (St. Louis, MO, USA). A luciferase reporter construct for the SLUG promoter was obtained from Dr. Yibin Kang (Princeton University). Lipofectamine-2000 and Fugene-6 were procured from Invitrogen (CA, USA) and Promega Corporation (WI, USA), respectively. Dharmafect-4 transfection reagent was obtained from Dharmacon (Lafayette, CO, USA). Lysophosphatidic acid (LPA) and actinomycin-D were purchased from and Sigma (St. Louis, MO, USA) respectively. Micro-RNA inhibitor (Anti-miR145-5p) and corresponding negative control (NC1) were purchased from Integrated DNA Technologies (San Diego, CA, USA).

**Cells**: The human breast cancer cell line SUM-1315 was obtained from Dr. Stephen Ethier (Medical University of South Carolina). MDA-435, MDA-231, Hs578t, SKBR3 and HEK293T cell lines were obtained from American Type Culture Collection (ATCC). These cell lines were authenticated using the University of Arizona Genetics Core. IMP3, SLUG, TAZ and WNT5B-

depleted cell lines were generated by infecting cells with pLKO.1 based lentiviruses expressing the corresponding shRNAs and subsequent selection in puromycin (1-2µg/mL). IMP3 and SLUG expression constructs were generated as described previously (Samanta et al., 2016). A WNT5B expression vector (pCDNA-WNT5B #35912) was purchased from Addgene (Cambridge, MA). Transient transfection of IMP3, SLUG and WNT5B was performed using Fugene-6 reagent. An shRNA resistant IMP3-expression construct was generated as described previously (Samanta et al., 2013). A constitutively active TAZ expression vector (4SA-TAZ) was obtained from Dr. Bob Varelas (Boston University). Transfection of anti-miR145-5p was performed using Dharmafect-4 transfection reagent.

IMP3-specific guide RNAs (gRNA) were designed using the CHOPCHOP (https://chopchop.rc.fas.harvard.edu/) and cloned into Lenti-CRISPR-V2 plasmid (Addgene # 52961) following the published protocol (Sanjana et al., 2014; Shalem et al., 2014). Subsequent production of lentiviral particles of the gRNAs and transduction into the cells followed by puromycin selection was performed as mentioned elsewhere. A scrambled gRNA was also designed and used as control. The gRNA sequences are listed in Table S3.

**RNA-sequencing analysis:** RNA-sequencing analysis was performed using total RNA extracted form control (shControl) and IMP3-depleted SUM-1315 cells. IMP3 was depleted using two different shRNAs (shIMP3-1 and shIMP3-2) and each sample was prepared in duplicate. Sequencing was performed using Illumina HiSeq-2000 instrument in the deep sequencing core facility at University of Massachusetts Medical School. The sequencing library that was prepared from total RNA by the core facility can be used to detect mRNA, small RNAs and long-non-coding RNAs. Raw reads were trimmed to remove the first 20 nucleotides using fastx_toolkit (v.0.0.14) followed by alignment to the reference human genome (hg19) using TopHat (v.2.0.9) (Kim et al.,

2013) with the following parameters: " -G [ucsc_hg19_knownGene] --b2-very-sensitive". The hg19 annotation file was downloaded from https://support.illumina.com/sequencing/sequencing_software/igenome.html, which contains both protein coding genes and miRNAs. Differential gene expression analysis was performed using Cufflinks (v2.2.1) (Trapnell et al., 2013).

**Gene set enrichment analysis:** Gene Set Enrichment Analysis (GSEA (Baas et al., 2006; Laudanski et al., 2006; Palacios et al., 2007; Pasieka et al., 2006; Subramanian et al., 2005) was performed using conserved YAP/TAZ target gene set available from molecular Signatures Database (version 6.1) (MolSigDB, http://software.broadinstitute.org/gsea/msigdb/index.jsp). The FPKM (Fragments Per Kilobase of transcript per Million mapped reads) values of all genes calculated by cuffdiff and were imported into GSEA. GSEA was performed separately for shIMP3-1 and shIMP3-2 compared to control cells (shGFP).

**cBioPortal data processing:** The mRNA expression data of human breast cancer samples was downloaded from cBioPortal for Cancer Genomics and Pearson's correlation analysis was performed to calculate correlation coefficient (*p*). The cBioportal data are expressed as Z-Scores, which is the relative expression of an individual gene in a tumor sample to the expression distribution of that gene in a reference population. The reference population is all of the samples that are diploid for the gene in question. The Z-score indicates the number of standard deviations away from the mean of expression in the reference population, which can be positive or negative. This measure is useful to determine whether a gene is up- or down-regulated relative to the normal samples or all other tumor samples.

## References


Baas, T., Baskin, C.R., Diamond, D.L., Garcia-Sastre, A., Bielefeldt-Ohmann, H., Tumpey, T.M., Thomas, M.J., Carter, V.S., Teal, T.H., Van Hoeven, N., *et al.* (2006). Integrated molecular signature of disease: analysis of influenza virus-infected macaques through functional genomics and proteomics. J Virol *80*, 10813-10828.

Kim, D., Pertea, G., Trapnell, C., Pimentel, H., Kelley, R., and Salzberg, S.L. (2013). TopHat2: accurate alignment of transcriptomes in the presence of insertions, deletions and gene fusions. Genome Biol *14*, R36.

Laudanski, K., Miller-Graziano, C., Xiao, W., Mindrinos, M.N., Richards, D.R., De, A., Moldawer, L.L., Maier, R.V., Bankey, P., Baker, H.V., *et al.* (2006). Cell-specific expression and pathway analyses reveal alterations in trauma-related human T cell and monocyte pathways. Proc Natl Acad Sci U S A *103*, 15564-15569.

Palacios, R., Goni, J., Martinez-Forero, I., Iranzo, J., Sepulcre, J., Melero, I., and Villoslada, P. (2007). A network analysis of the human T-cell activation gene network identifies JAGGED1 as a therapeutic target for autoimmune diseases. PLoS ONE *2*, e1222.

Pasieka, T.J., Baas, T., Carter, V.S., Proll, S.C., Katze, M.G., and Leib, D.A. (2006). Functional genomic analysis of herpes simplex virus type 1 counteraction of the host innate response. J Virol *80*, 7600-7612.

Samanta, S., Pursell, B., and Mercurio, A.M. (2013). IMP3 protein promotes chemoresistance in breast cancer cells by regulating breast cancer resistance protein (ABCG2) expression. The Journal of biological chemistry *288*, 12569-12573.

Samanta, S., Sun, H., Goel, H.L., Pursell, B., Chang, C., Khan, A., Greiner, D.L., Cao, S., Lim, E., Shultz, L.D., *et al.* (2016). IMP3 promotes stem-like properties in triple-negative breast cancer by regulating SLUG. Oncogene *35*, 1111-1121.

Sanjana, N.E., Shalem, O., and Zhang, F. (2014). Improved vectors and genome-wide libraries for CRISPR screening. Nature methods *11*, 783-784.

Shalem, O., Sanjana, N.E., Hartenian, E., Shi, X., Scott, D.A., Mikkelson, T., Heckl, D., Ebert, B.L., Root, D.E., Doench, J.G., *et al.* (2014). Genome-scale CRISPR-Cas9 knockout screening in human cells. Science *343*, 84-87.

Subramanian, A., Tamayo, P., Mootha, V.K., Mukherjee, S., Ebert, B.L., Gillette, M.A., Paulovich, A., Pomeroy, S.L., Golub, T.R., Lander, E.S., *et al.* (2005). Gene set enrichment analysis: a knowledge-based approach for interpreting genome-wide expression profiles. Proc Natl Acad Sci U S A *102*, 15545-15550.

Trapnell, C., Hendrickson, D.G., Sauvageau, M., Goff, L., Rinn, J.L., and Pachter, L. (2013). Differential analysis of gene regulation at transcript resolution with RNA-seq. Nat Biotechnol *31*, 46-53.